# An Origami-Inspired Deployable Space Debris Collector

Yuto Tanaka, Aditya Arjun Anibha, Leonard Jung, Roha Gul, Jeffrey Sun, and Ran Dai

Abstract—This paper develops a novel approach to design, actuate, and manufacture a space debris collector based on the conical Kresling origami pattern. The deployable nature of origami structures and the radial closability of the conical Kresling pattern are leveraged to form an enclosure volume for collecting space debris at different sizes. We first introduce the geometric, volume, and energy models of the conical Kresling pattern. Based on these models, the debris collector design problem is formulated as a parameter optimization problem to minimize the actuation energy for the folding process while satisfying the minimum volume constraint and geometric/functional constraints. To automatically capture debris in space, an actuation system is designed, which is compatible with space environments. Moreover, the multi-material three-dimensional printing technology is applied to build the designed debris collector, which makes it feasible for manufacturing the product in orbit. The proposed design, actuation, and manufacturing approaches are verified with experimental tests using a designed prototype.

Index Terms—Space Robots, Origami-Inspired Deployable System, Debris Connector, Optimal Design

# I. INTRODUCTION

The amount of space debris surrounding Earth is growing exponentially due to human's continuous space exploration activities. If left unchecked, it will significantly increase the risk attached to space travel and operations, particularly in low Earth orbit. Several approaches have been developed to mitigate this issue, all focusing on deorbiting the debris, such as tethers and harpoons [1], laser ion-beams [2], deployable smallsats [3], net capture, and robotic arms [4]. Tethers and harpoons attach a parent control satellite to the debris to pull it out of orbit. A laser ion beam is used to impart an ablative effect on one surface of debris to create a propulsion force to deorbit it. Deployable smallsats with propulsion capabilities inside a carrier spacecraft rendezvous with the debris and then attach to it for deorbiting. Net captures and robotic arms involve the deployment of nets or robotic arms to wrap and clamp around the debris to drag it out of orbit. However, these concepts have common limitations which prevent them from reducing space debris at different sizes, ranging from 1 millimeter to above 1 meter. The large quantity of space

This research is supported in part by NSF grant CPS-2201568. Yuto Tanaka, Aditya Anibha, Leonard Jung, Roha Gul, and Ran Dai are with the School of Aeronautics and Astronautics, Purdue University, West Lafayette, IN, 47907. Jeffrey Sun is with West Lafayette High School. Emails: tanaka9, aanibha, rgul, jung340, and randai@purdue.edu

debris indicates that a high quantity of these debris collectors is required, which means they need to be manufactured in orbit to collect all of them, especially if the collector is not a reusable design. Because of their large-volume usage, they would need multiple launches for delivering large-volume instruments to space. Failed collectors can add to space debris if they collide with it and cannot absorb impacts. A more efficient and in-orbit manufacturable debris collection system is required that can be folded for space-saving and deployed multiple times on demand.

Origami-Inspired Foldable Space Debris Collectors solve these disadvantages as they can fold into a small space to save payload space allowing multiple to be launched and deployed at once, collect debris several times, and absorb impacts due to their flexibility. They can expand to accommodate more debris storage and vary their structure to mechanically lock debris in place using Origami apertures. Every space launch has a high cost associated with limited mass and volume.

Origami transforms a flat sheet of paper into a threedimensional (3D) sculpture by folding along creases in a designed pattern. The fusion of engineering technology, mathematical principles, and intricate design of origami patterns has led to the explosive growth of origami-inspired applications in architecture [5], aerospace [6], [7], robotics [8], and medical devices [9]. Among them, origami structures have gained massive attention and demonstrated great potential in existing and future space-related applications. Since every single space launch has a high cost associated with limited mass and volume, a deployable system that is able to adapt its shape or function in-situ will address the challenges of high volume and mass demands in future space operations. Representative scenarios where an origami structure plays a critical role in space operations include foldable solar panels and inflatable habitat rooms for astronauts in space. The advantages of origami structure motivate the development of an origami-inspired deployable space debris collector for space saving and multi-time usage.

Typical origami patterns include Yoshimura, Miura, Kresling, Waterbomb, and Resch [10]. Kresling is a foldable pattern created when a thin cylindrical shell is subjected to torsion [11]. Twisting and folding the Kresling structure creates a diaphragm perpendicular to the tube axis. Kresling panels can be rigid enough to withstand the load compared with the iris flexible sleeves, and the fully folded state of Kresling is stable without any panel deformation. However, the folding process of the structure causes panel deformation, leading to strain energy. The radial closability of the Kresling structure can be used to collect space debris. Since the

traditional Kresling pattern can be radially closed under one special case due to its structure limitation [12], the conical Kresling pattern [13], with an increased degree of freedom, becomes a more appropriate pattern for constructing a space debris collector. In addition to its space-saving characteristics, the Kresling pattern is known for absorbing the energy impacted from a specific direction and allowing the system to trap the debris in an enclosed space efficiently.

Since energy consumption is always a concern for space operations, the design of the Kresling origami structure not only considers the enclosure volume for capturing and keeping the debris, but also minimizes the energy required for folding/unfolding the origami structure. The functional operation of an origami-inspired system requires a well-controlled actuation system. Although traditional actuation mechanisms such as magnetic [14] and pneumatic [15] actuators have been adopted in Earth environments, they are not practical in space environments considering the extreme temperature and lack of infrastructure to deploy these mechanisms. To realize autonomous folding and deployment onboard, an energy-efficient Kresling pattern-based space debris collector with an equipped actuation system will be developed.

Historically, origami structures in engineering require a blend of both rigid and soft materials to allow for smooth actuation, freedom of motion, and structural stability. For applications involving solar arrays, rigid plastics or metals are used for panel areas, and softer materials such as cloths are used for hinge areas to allow easy bending [16]. However, fabricating these structures is time-consuming. It requires not only individual manufacturing of each major component but also manual assembly of all components. In the interest of rapid, low-cost fabrication, the focus has been shifted to computer-aided processes, such as lithographic, two-dimensional (2D) printing, and laser-cut designs [17]. In particular, 3D printing of 2D planar designs allows for both a one-step assembly of the robotics structure and easy integration of robot actuators. For instance, [17] first demonstrated 'printable robotics' with a folding 2D laserengraved structure and shape-memory alloy (SMA) actuators. Work in [18] successfully explored integrating shapememory polymers into a 2D planar design for autonomous, self-folding systems. With a multi-material 3D printer, [19] demonstrated and validated a novel method to fully print a complex 3D structure in a single print.

Inspired by the advantages of conical Kresling patterns, we propose a foldable space debris collector that is composed of multi-layer conical Kresling structures. These layers can be deployed and folded in sequence, which makes it feasible for trapping the captured debris while having other layers open for successive collections. In addition, an autonomous actuation system is designed to enable full autonomy of the folding/unfolding process. Moreover, the design accommodates the in-orbit manufacturable requirement, which allows the origami structure to be manufactured by a multi-material 3D printer. The overall design incorporating structure optimization, actuation, and manufacturing leads to a novel space

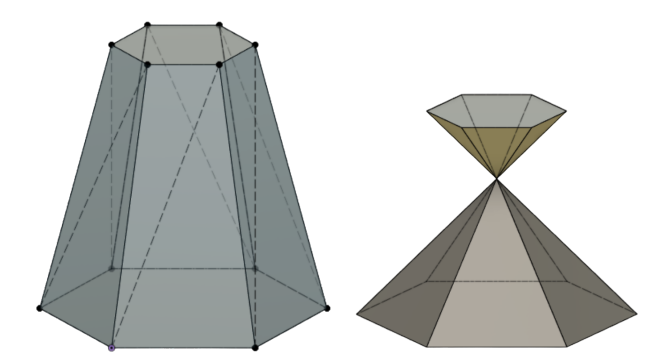
debris collection system that will have a high impact on the space safety field.

The paper is organized as follows. §II describes the models of the Kresling origami and the formulation of the design problem. §III presents the prototype manufacturing, including the actuation system and multi-material 3D printing. The simulation and experimental results are presented in §IV. Lastly, the conclusions and future work are addressed in §V.

# II. OPTIMAL DESIGN OF DEBRIS COLLECTOR BASED ON CONICAL KRESLING PATTERN

#### A. Geometric Model

The conical Kresling pattern is described by a set of parameters that have coupling constraints to create a foldable structure. These parameters work together to define the shape, size, and folding states of a conical Kresling origami. As shown in Fig. 1b, when fully folded, the bottom part generates an enclosure volume that can be used to store the collected debris, while the top part can work as a valve to seal the collected debris in the bottom part. These features meet the requirements of a deployable debris collector, which allows a fully deployed state (Fig. 1a) to be hollow for capturing debris and its folded state (1b) to form an enclosure volume. The geometric model for the conical Kresling pattern is introduced below.

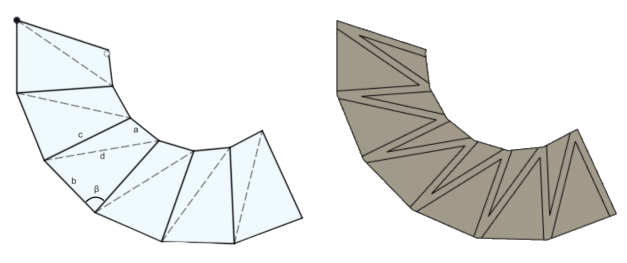


(a) Deployed conical Kresling (b) Folded conical Kresling structure state (State 1) structure state (State 2)

Fig. 1: Example of a conical Kresling structure with two stable states ( $a=1,\,b=2,\,c=4,\,\beta=1.45\,rad$ )

The unit of a Kresling pattern is a convex quadrilateral cell. The parameters used to define a Kresling unit cell are shown in Fig. 2a. The four key parameters are a, b, c, and  $\beta$ , where a, b, c represent the length of the quadrilateral sides, and  $\beta$  is the angle between sides c and b. The length of the diagonal d is determined by a, b, c, and  $\beta$ , expressed as  $d = \sqrt{b^2 + c^2 - 2bc\cos(\beta)}$ . The side labeled by c is the mountain crease, and the diagonal labeled by d is the valley crease. The geometric model needs to be adjusted by implementing a hinge to create foldable parts of each unit cell, as shown in Fig. 2b. By folding along the mountain/valley creases in a repeated manner and connecting the two ends, it forms a Kresling origami, shown in Fig. 1. The top view of the folded control Kresling structure is

The top view of the folded conical Kresling structure is shown in Fig. 3. The vertices of the top and bottom surfaces are located on two circumcircles. The radii of the top and



(a) Model with Parameters

(b) Model with hinges

Fig. 2: Geometric model of conical Kresling pattern

bottom circumcircle, denoted by r and R, respectively, are calculated by

$$r = \frac{a}{2\sin(\frac{\pi}{n})}, \ R = \frac{b}{2\sin(\frac{\pi}{n})} \tag{1}$$

where n is the number of unit cells. By denoting the perimeter length of the top polygon as l, we have

$$a = \frac{l}{n}. (2)$$

By twisting the Kresling, it drives the structure to fold. The twist angle, denoted by  $\phi$ , is the relative rotation angle of the bottom to the top surface, as shown in Fig. 3. The twist angle must follow  $0 \le \phi \le \pi - \frac{2\pi}{n}$ , where  $\phi_{max} = \pi - \frac{2\pi}{n}$  is when the valley crease lines intersect each other. In other words, when  $\phi = \phi_{max}$ , the valley crease lines intersect at one point when fully folded such that they generate an enclosure volume, e.g., the bottom section in Fig. 1b. This important feature will be used to design the debris collector.

During folding, the lengths of mountain and valley creases will be affected by the twist angle, expressed as

$$\tilde{c}(h,\phi) = \sqrt{h^2 + r^2 + R^2 - 2rR\cos(\phi)}$$
 (3a)

$$\tilde{d}(h,\phi) = \sqrt{h^2 + r^2 + R^2 - 2rR\cos(\phi + \frac{2\pi}{n})}$$
 (3b)

where  $h(\phi)$  is the height of the Kresling at any state. More details of the Kresling model can be referred to [13].

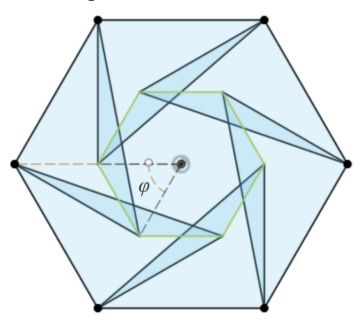


Fig. 3: Twist Angle Displayed on Conical Kresling Pattern

#### B. Volume Model

The shape of the conical Kresling pattern can be regarded as a regular polygon frustum, as shown in Fig. 1a. The volume of a frustum is determined by

$$V = \frac{h}{3}(A_1^2 + \sqrt{A_1 A_2} + A_2^2) \tag{4}$$

where  $A_1$  and  $A_2$  is the area of the top and bottom plane, respectively, and h is the height of the structure. From the calculation of the area of regular polygons, the volume of the conical Kresling pattern in state 1 is expressed as

$$V_1 = \frac{nh}{12}\cot\left(\frac{\pi}{n}\right)(a^2 + ab + b^2). \tag{5}$$

When using the designed conical Kresling structure as a debris connector, the volume of the origami will be considered for capturing a specific target. The volume expression in (5) is a highly nonlinear function that is determined by several pattern parameters. For a given target to be captured by a debris collector, we expect the volume of the designed origami is above a minimum value to host the target inside.

### C. Energy Model

Since there is panel deformation during folding for a Kresling origami, the elastic energy is used as the strain energy required for folding, which is determined by

$$U = \frac{nk_m}{2}(c - \tilde{c}(h, \phi))^2 + \frac{nk_v}{2}(d - \tilde{d}(h, \phi))^2$$
 (6)

where  $k_m$  and  $k_v$  are the stiffness coefficients of the mountain and valley creases, respectively. The plots of the strain energy with respect to the height for a set of b values are shown in Fig. 4.

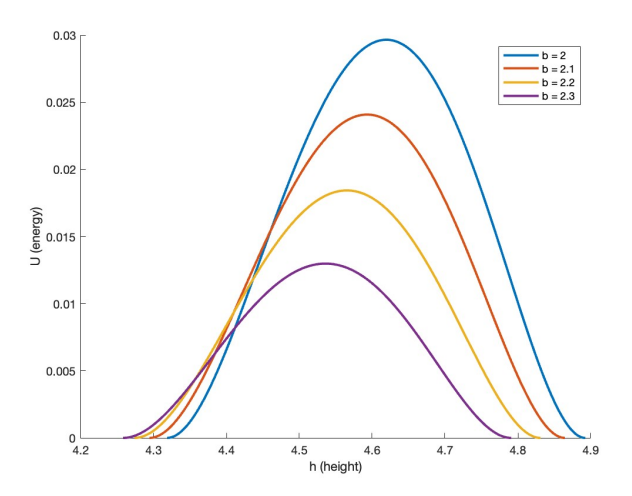


Fig. 4: Strain energy as a function of h, where a=1, c=5, n=6, and  $\beta=1.5$  rad.

By setting the derivatives of the strain energy in (6) to be zero, it yields three solutions, which implies three stable cases, where each case is also radially closable. One is the mono-stable case, where the conical Kresling pattern does not fold and is only stable under one special state. The other two are the bi-stable cases, with one stable state and one quasi-stable state. The quasi-stable state requires a constant input of energy to maintain its stability, which is not practical for an autonomous debris collector. Hence, the bi-stable case with two stable states will be used to design the structure of a debris collector.

For the bi-stable case with two stable states,  $\phi$  and h at the two states are determined by solving  $\partial U/\partial h=0$  and  $\partial U/\partial \phi=0$ , which yields

$$\phi_1 = \arcsin(\lambda) - \frac{\pi}{n} \tag{7a}$$

$$\phi_2 = \pi - \arcsin(\lambda) - \frac{\pi}{n} \tag{7b}$$

$$h_1 = \sqrt{c^2 - r^2 - R^2 + 2rR\cos(\phi_1)}$$
 (7c)

$$h_2 = \sqrt{c^2 - r^2 - R^2 + 2rR\cos(\phi_2)}$$
 (7d)

where  $\lambda=\sin(\phi+\frac{\pi}{n})=\frac{b-2c\cos(\beta)}{a}sin\frac{\pi}{n}.$  Since  $0\leq\phi\leq\pi-\frac{2\pi}{n}$  due to the geometric constraint,  $\lambda$  is then constrained by  $\sin(\frac{\pi}{n})\leq\lambda<1.$  To form an enclosure volume for the debris collector when fully folded, such as the example in Fig. 1b, the radial closability requires  $\phi_2=\phi_{max},$  which indicates the max twist angle for the fully folded state make the crease lines intercept at one point [12]. When  $\phi_2=\phi_{max},$  we have  $\lambda=\sin(\frac{\pi}{n}),$  which leads to the geometric constraint

$$b - 2c\cos(\beta) = a \tag{8}$$

for radial closability. By inserting  $\lambda = sin(\frac{\pi}{n})$  into the  $\phi_1$  expression in (7a), the radial closability also leads to  $\phi_1 = 0$ , as shown in the example of Fig. 1a. Therefore, the bi-stable case with two stable states of the conical Kresling origami is utilized for the debris collector's capturing and sealing purposes, e.g., State 1 in Fig. 1a for capturing debris when unfolded; and State 2 in Fig. 1b for enclosing the captured debris within the collector when fully folded.

When folding between the two stable states, the strain energy in Fig. 4 demonstrates a parabolic shape curve. To find the total energy consumed during the folding process, the integral of the strain energy in (6) from one stable state, represented by the initial twist angle  $\phi_1$ , to the other stable state, represented by the final twist angle  $\phi_2$ , will be computed. Since the energy consists of two independent variables, linear interpolation of h in terms of  $\phi$  is applied between the two stable states, which yields  $\tilde{h}(\phi) \approx h$ . Then, the total energy consumed during the folding process is expressed as

$$\begin{split} \Sigma U &= \int_{\phi_1}^{\phi_2} [\frac{k_v n}{2} (\sqrt{\tilde{h}(\phi)^2 + r^2 + R^2 - 2rR\cos(\phi)} - c)^2 \\ &+ \frac{k_m n}{2} (\sqrt{\tilde{h}(\phi)^2 + r^2 + R^2 - 2rR\cos(\phi + \frac{2\pi}{n})} - d)^2] d\phi. \end{split}$$

As energy consumption is always a concern for spacerelated operations, the strain energy used for folding/unfolding the conical Kresling based debris collector from one stable state to the other will be used as a performance index when designing the debris collector's structure. With the objective defined by the energy model, the geometric and volume models act as constraints to make the Kresling origami physically and functionally feasible when optimizing the objective function.

#### D. Formulation of the Optimal Design Problem

To design a debris collector that captures debris objects with a lower bounded volume, denoted by  $V_{min}$ , while minimizing the energy required for actuating debris collector folding/unfolding process, the design problem is formulated as a parameter optimization problem subject to a set of constraints. The problem formulation is as follows:

$$\min_{b,c,n,\beta} \Sigma U \tag{9a}$$

s.t. 
$$a = \frac{l}{n}, \ r = \frac{a}{2\sin(\frac{\pi}{n})}, \ R = \frac{b}{2\sin(\frac{\pi}{n})}$$
 (9b)

$$d = \sqrt{b^2 + c^2 - 2bc(\cos(\beta))}$$
 (9c)

$$\phi_1 = \arcsin(\lambda) - \frac{\pi}{n} \tag{9d}$$

$$\phi_2 = \pi - \arcsin(\lambda) - \frac{\pi}{n} \tag{9e}$$

$$h_1 = \sqrt{c^2 - r^2 - R^2 + 2rR\cos(\phi_1)}$$
 (9f)

$$h_2 = \sqrt{c^2 - r^2 - R^2 + 2rR\cos(\phi_2)}$$
 (9g)

$$\lambda = \frac{b - 2c\cos(\beta)}{a}\sin\left(\frac{\pi}{n}\right) \tag{9h}$$

$$0 \le \phi_1 \le \pi - \frac{2\pi}{n}, \ h_1 \ge 0$$
 (9i)

$$0 \le \phi_2 \le \pi - \frac{2\pi}{n}, \ h_2 \ge 0$$
 (9j)

$$b - 2c\cos(\beta) = a \tag{9k}$$

$$V_1 \ge V_{min} \tag{9l}$$

where the objective is to minimize the total strain energy during the folding process. The constraint set includes the geometric constraints (9b)-(9c), the two stable states for starting and ending the folding process (9d)-(9h), the associated stable state constraints (9i)-(9j), the radial closability constraint (9k), and the minimum volume constraint (9l). Since parameter a can be considered as a normalized value by setting the perimeter length of the top polygon as l as a unit value, a is taken as a given parameter.

The parameter optimization problem formulated in (9) includes both continuous variables, i.e., b, c,  $\beta$ , and an integer variable, n, and the constraints are nonlinear. Therefore, problem (9) is classified as a mixed-integer nonlinear programming (MINLP) problem, which is NP-hard. A commercial MINLP solver, which combines sequential quadratic programming and the branch-and-bound method, is applied to solve the formulated design problem.

#### III. PROTOTYPE MANUFACTURING

# A. Actuation System

The actuation system leverages the tethered rotational servos to drive the folding process. As shown in Fig. 5, a set of 360-degree freely rotating servos are attached to alternate internal panels to actuate the prototype. These servos reel in a string connected to an adjacent panel without a servo. The holes added to the panels, as shown in Fig. 6, allow the strings to pass through the panels, such that the adjacent panels will be connected when the string is tethered. Using tension, the servo rotation pulls the string and the two

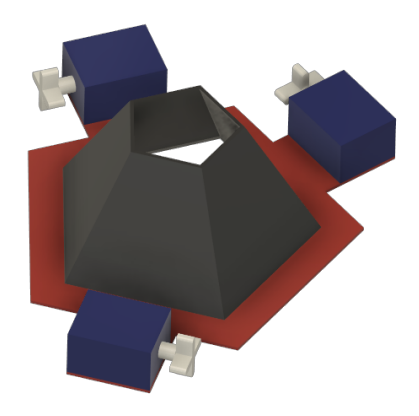


Fig. 5: Placement of rotating servos for actuation

adjacent panels together. This leads to all the panels folding naturally into a closed configuration. The servos are placed on alternate panels to reduce the complexity that comes with an excessive number of motors while creating radially symmetrical forces to fold the origami evenly. The design was made using a combination of rigid panels and flexible hinges. Offsets of approximately 1-2 mm were added at the hinges to allow freedom of movement for the rigid panels. Due to the thickness of the origami, it physically cannot attain its full folding state. Thus, a manufacturing tolerance needs to be considered when compared to the ideal design results.

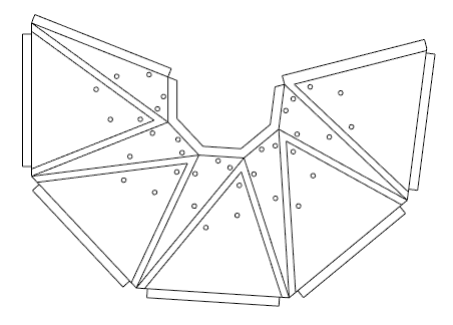


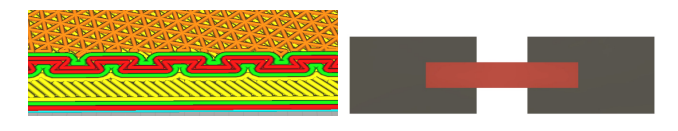
Fig. 6: Holes on the modified conical Kresling pattern to allow the string to pass panels

To transform into the open configuration, the servos are rotated in the opposite direction to unreel the strings and reduce the applied tension on the panels. Since the hinges are originally 3D printed in a flat pattern, they tend to resist any force that causes them to fold. Hence, the natural elastic resistance of the hinges causes the origami to unfold by itself. The hinges must be made thick enough to ensure they are sufficient to overcome the structure's own weight, but must remain within reasonable manufacturing tolerance so that it can attain as close as possible to a closed configuration.

# B. Multi-material 3D-printing

For manufacturing the Kresling origami, a dual-extrusion 3D printer is used to print two layers of materials, allowing for both flexibility of hinges and ridigity of panels. The first layer printed is a plane of flexible Thermoplastic Polyurethane (TPU) plastic to serve as the hinges. A thicker, second layer of Polylactic acid (PLA) plastic is printed

over the TPU plane to serve as rigid faces. By using a dual-extrusion printer, minimal assembly is required, as the two plastics are printed together in one singular print. The resulting print is merged at its hinges to create the Kresling pattern. To ensure rigid joints between the PLA and TPU, a dovetail overlay was used across the intersecting sides (Fig. 7a). The layer of TPU was sandwiched equally between the PLA faces to allow for symmetric bidirectional folding (Fig. 7b). Using this method, designs can be rapidly prototyped and tested. The 3D printing approach of the Kresling origami also makes it feasible for in-orbit manufacturing the designed debris collector.



(a) Dovetail Joint (b) Sandwich Design Fig. 7: Joint design for PLA (black) and TPU (red)

#### IV. SIMULATION AND EXPERIMENTAL RESULTS

#### A. Simulation Results

This section demonstrates simulation results for designing a specific debris collector with its minimum volume at stable state 1 constrained by  $V_{min}=40~{\rm mm}^3$ . In addition, to use the conical Kresling pattern to create a foldable debris collector, certain design considerations are made. First, a lower and upper bound is given to the number of unit cells  $5 \le n \le 12$  to ensure easy folding and reduce the complexity of the structure. Second, the height of the structure at stable state 2 is given an upper and lower bound  $0.01 \le h_2 \le 0.1$  mm so that the designed structure can be fully folded flat. Moreover, parameter a is normalized by setting  $l=6~{\rm mm}$ .

The optimal design problem in (9) is solved using a commercial MINLP solver [20]. Since the problem is highly nonlinear, solutions obtained from the MINLP solver are locally optimal, which indicates global optimality is not guaranteed. To search for a global optimal solution for the formulated MINLP problem, a heuristic approach is integrated with the MINLP solver. The heuristic approach involves a set of cases solved corresponding to random initial guesses in order to find the best local optimal solution for prototyping. 500 different sets of initial guesses for all design variables are randomly generated with the ranges set as  $b \in [1 5]$  mm,  $c \in [1 5]$  mm,  $n \in [5 12]$ , and  $\beta \in \begin{bmatrix} \frac{\pi}{4} & \pi \end{bmatrix}$  rad. After solving all 500 cases using the MINLP solver, 498 cases converge, from which 383 converge to the same optimum. This optimum point gives the lowest energy out of all solutions while satisfying all constraints. Hence, the final design variable values are selected at this optimum point, b = 4.072mm, c = 3.904mm, n = 5,  $\beta = 1.194$  rad.

# B. Experimental Tests

Using the design results obtained from  $\S$ IV-A, we manufactured the prototype according to the method discussed in  $\S$ III. Since the design results shown in  $\S$ IV-A are normalized by setting l=6 mm, the size of the prototype for the

experiment is multiplied by 20. Since the theoretical model is considered with negligible thickness, there is a degree of freedom within the twist angle for the prototype to consider the thickness of the panels. The prototype folds effectively with precise control of the phase of folding. When it is fully folded, the internal creases intercept, which leads to an enclosure volume. The speed of the folding process can also be controlled by the rotational speed of the motors. Figures 8c and 8d demonstrate the manufactured prototype under the fully folded and unfolded states, respectively. The folding process is recorded in the attached video clip. The demo here provides one layer of the debris collector. Since each layer can be repeated and connected in sequence, and the folding process of each layer is independent of the others, it is feasible to have a multi-layer debris collector for successive debris collection.

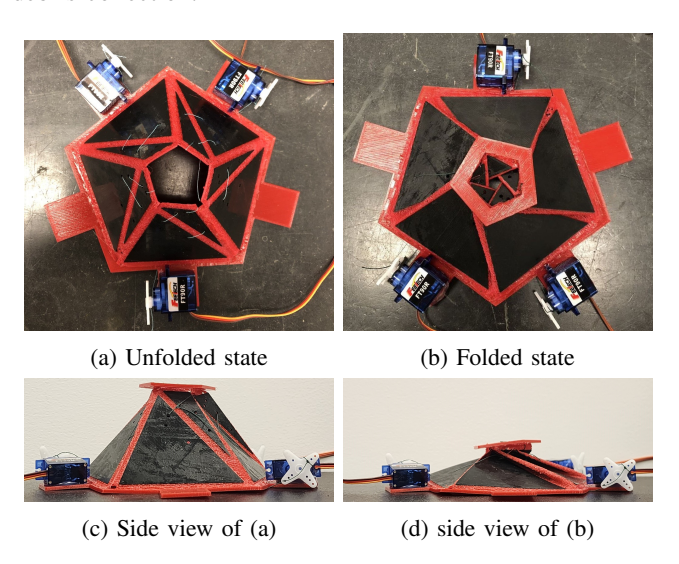


Fig. 8: Experimental demo of the designed debris collector at folded and unfolded states

# V. CONCLUSION

This paper develops an integrated approach for designing, actuating, and manufacturing a space debris collector based on the conical Kresling origami pattern. The design finds an optimized Kresling structure by minimizing the actuation energy requirement and meeting the minimum volume constraint for capturing a specific debris object with a given volume. In addition, the designed structure meets the geometric constraints to form an enclosure volume when fully folded to lock captured debris. The prototype is 3D printed using a combination of Thermoplastic Polyurethane (TPU) and Polylactic acid (PLA) materials to emulate the flexibility of origami while maintaining rigid panels. The folding process is actuated using tethered servos to allow precise control throughout the folding process. The resulting design successfully demonstrates the functionality of the conical Kresling origami based debris collector. More importantly, this novel product demonstrates advantages in terms of being easily manufacturable, flexible, compressible or expandable across a large range of volume, and adaptable to absorb impacts. The proposed space debris collector can be attached to the spacecraft for deployment upon request. They can also actively chase space debris when equipped with a propulsion system. Further work will investigate the use of a bidirectional actuation system to support the unfolding process and physically testing the multi-layer conical Kresling structure's capabilities in debris collection.

#### REFERENCES

- V. Aslanov and V. Yudintsev, "Dynamics of large space debris removal using tethered space tug," *Acta Astronautica*, vol. 91, p. 149–156, 2013
- [2] R. Soulard, M. N. Quinn, T. Tajima, and G. Mourou, "Ican: A novel laser architecture for space debris removal," *Acta Astronautica*, vol. 105, no. 1, p. 192–200, 2014.
- [3] H. Hakima, M. C. Bazzocchi, and M. R. Emami, "A deorbiter cubesat for active orbital debris removal," *Advances in Space Research*, vol. 61, no. 9, p. 2377–2392, 2018.
- [4] M. Shan, J. Guo, and E. Gill, "Review and comparison of active space debris capturing and removal methods," *Progress in Aerospace Sciences*, vol. 80, p. 18–32, 2016.
- [5] A. E. Del Grosso and P. Basso, "Adaptive building skin structures," Smart Materials and Structures, vol. 19, no. 12.
- [6] S. A. Zirbel, R. J. Lang, M. W. Thomson, D. A. Sigel, P. E. Walke-meyer, B. P. Trease, S. P. Magleby, and L. L. Howell, "Accommodating thickness in origami-based deployable arrays," *Journal of Mechanical Design*, vol. 135, no. 11, 2013.
- [7] K. Miura, "Map fold a la miura style, its physical characteristics and application to the space science," pp. 77–90, 1994.
- [8] S. Felton, M. Tolley, E. Demaine, D. Rus, and R. Wood, "A method for building self-folding machines," *Science*, vol. 345, no. 6197, pp. 644–646, 2014.
- [9] G. V. Rodrigues, L. M. Fonseca, M. A. Savi, and A. Paiva, "Nonlinear dynamics of an adaptive origami-stent system," *International Journal* of Mechanical Sciences, vol. 133, pp. 303–318, 2017.
- [10] D. Dureisseix, "An overview of mechanisms and patterns with origami," *International Journal of Space Structures*, vol. 27, no. 1, pp. 1–14, 2012.
- [11] C. Jianguo, D. Xiaowei, Z. Ya, F. Jian, and T. Yongming, "Bistable behavior of the cylindrical origami structure with kresling pattern," *Journal of Mechanical Design*, vol. 137, no. 6, p. 061406, 2015.
- [12] S. Ye, P. Zhao, Y. Zhao, F. Kavousi, H. Feng, and G. Hao, "A novel radially closable tubular origami structure (rc-ori) for valves," in *Actuators*, vol. 11, no. 9. MDPI, 2022, p. 243.
- [13] L. Lu, X. Dang, F. Feng, P. Lv, and H. Duan, "Conical kresling origami and its applications to curvature and energy programming," *Proceedings of the Royal Society A*, vol. 478, no. 2257, 2022.
- [14] M. Sivaperuman Kalairaj, C. J. Cai, and H. Ren, "Untethered origami worm robot with diverse multi-leg attachments and responsive motions under magnetic actuation," *Robotics*, vol. 10, no. 4, p. 118, 2021.
- [15] R. V. Martinez, C. R. Fish, X. Chen, and G. M. Whitesides, "Elastomeric origami: programmable paper-elastomer composites as pneumatic actuators," *Advanced functional materials*, vol. 22, no. 7, pp. 1376–1384, 2012.
- [16] S. A. Zirbel, R. J. Lang, M. W. Thomson, D. A. Sigel, P. E. Walkemeyer, B. P. Trease, S. P. Magleby, and L. L. Howell, "Accommodating Thickness in Origami-Based Deployable Arrays1," *Journal of Mechanical Design*, vol. 135, no. 11, 2013.
- [17] C. D. Onal, R. J. Wood, and D. Rus, "Towards printable robotics: Origami-inspired planar fabrication of three-dimensional mechanisms," in 2011 IEEE International Conference on Robotics and Automation, 2011, pp. 4608–4613.
- [18] S. Felton, M. Tolley, E. Demaine, D. Rus, and R. Wood, "A method for building self-folding machines," *Science*, vol. 345, no. 6197, pp. 644–646, 2014. [Online]. Available: https://www.science.org/doi/abs/10.1126/science.1252610
- [19] T. Liu, Y. Wang, and K. Lee, "Three-dimensional printable origami twisted tower: Design, fabrication, and robot embodiment," *IEEE Robotics and Automation Letters*, vol. 3, no. 1, pp. 116–123, 2018.
- [20] K. Holmström, A. O. Göran, and M. M. Edvall, "User's guide for tomlab/minlp," 2007.